

Electricity Storage in Biofuels: Selective Electrocatalytic Reduction of Levulinic Acid to Valeric Acid or γ -Valerolactone

Le Xin, Zhiyong Zhang, Ji Qi, David J. Chadderdon, Yang Qiu, Kayla M. Warsko, and Wenzhen Li[✉][a]

Herein, we report an effective approach to electricity storage in biofuels by selective electrocatalytic reduction of levulinic acid (LA) to high-energy-density valeric acid (VA) or γ -valerolactone (gVL) on a non-precious Pb electrode in a single-polymer electrolyte membrane electrocatalytic (flow) cell reactor with a very high yield of VA (>90%), a high Faradaic efficiency (>86%), promising electricity storage efficiency (70.8%), and a low electricity consumption ($1.5 \text{ kWh L}_{\text{VA}}^{-1}$). The applied potential and electrolyte pH can be used to accurately control the reduction products: lower overpotentials favor the produc-


tion of gVL, whereas higher overpotentials facilitate the formation of VA. A selectivity of 95% to VA in acidic electrolyte (pH 0) and 100% selectivity to gVL in neutral electrolyte (pH 7.5) are obtained. The effect of the molecular structure on the electrocatalytic reduction of ketone and aldehyde groups of biomass compounds was investigated. Whereas LA can be fully electroreduced to VA though a four-electron transfer, the C=O groups are only electroreduced to -OH by a two-electron-transfer process when glyoxylic acid and pyruvic acid serve as feedstocks.

Introduction

With major raw oil reserves declining and the world's population rapidly growing, green-minded people are forced to seek renewable energy sources, such as biomass, solar, wind, geothermal, and tidal powers to decrease our heavy dependence on fossil fuels.^[1] Renewable electricity based on photovoltaic and wind power, although attractive, has an intermittent nature that requires the development of efficient energy-storage devices. Several advanced electricity-storage techniques have been proposed at different research and development (R&D) stages to solve this issue;^[2] these include pumped-storage hydropower (PSH), compressed-air energy storage (CAES), batteries, supercapacitors, and flywheels. In general, they serve to capture electrical energy generated during off-peak hours and convert them into the forms of gravitational potential energy (with PSH), molecular potential energy (with CAES), electrical potential energy (with batteries and supercapacitors), or kinetic energy (with flywheels), and to release electrical energy during peak demand. Similarly, overproduced renewable electricity can be captured in the form of chemical potential energy; this can be achieved by employing electrocatalytic processes to convert abundant, cheap biomass-derived compounds into biofuel-related compounds with higher energy densities.

High-energy-density liquid transportation fuels are critically important to a mobile, dynamic, and sustainable society. Lignocellulosic biofuels derived from plant biomass are considered the most dominant renewable source of liquid fuels to replace depleting fossil fuel resources (i.e., petroleum, natural gas, etc.).^[3] Currently, lignocellulosic biomass resources are significantly cheaper than petroleum (\$15 per barrel of crude oil equivalent), abundant (equivalent energy content of 60% of our domestic crude oil consumption), and annually renewable. Therefore, they are expected to share a substantial portion of our future energy landscape.^[3a,4] The US Department of Energy (DOE) has identified the top ten abundant, inexpensive, biomass-derived compounds [ethanol, furans, glycerol, hydroxypropionic acid/aldehyde, isoprene, levulinic acid (LA), succinic acid, lactic acid, sorbitol, and xylitol].^[5] These compounds will constitute the primary building blocks for our future production of chemicals and fuels. Among them, LA can be produced in large amounts from lignocellulose through hydrolysis with dilute sulfuric acid; this is considered the most promising method in terms of cost, yield, and scalability. High yields of >60% can be achieved for the conversion of cellulosic materials to LA in sulfuric acid.^[6] BioMetics Inc. has reported that a large-scale plant can produce LA at a cost of only \$0.09–0.11 kg^{-1} through dilute sulfuric acid hydrolysis,^[3a] which is significantly cheaper than \$5 kg^{-1} for pure LA in the global market.^[7] LA, although considered a promising feedstock for biofuel production, has excess oxygen functionalities. Thus, new processes are needed to effectively remove oxygen in the hydroxyl, ketone, aldehyde, and carboxylic groups of LA or its derivatives [γ -valerolactone (gVL), valeric acid (VA), etc.] to up-

[a] L. Xin, Dr. Z. Zhang, J. Qi, D. J. Chadderdon, Y. Qiu, K. M. Warsko, Prof. Dr. W. Li
Chemical Engineering Department, Michigan Technological University
1400 Townsend Drive, Houghton, MI 49931 (USA)
Fax: (+1) 906-487-3213
E-mail: wzli@mtu.edu

 Supporting Information for this article is available on the WWW under <http://dx.doi.org/10.1002/cssc.201200765>.

grade them to high-energy-density transportation fuels (gasoline, jet, and diesel fuels) or fuel additives.

The hydrogenation of LA to gVL^[8] and VA^[9] using Pt-, Pd-, or Ru-based mono- or bi- functional catalysts, has been investigated through heterogeneous catalytic processes. Recently, Dumesic's group developed a new integrated heterogeneous catalytic system to convert gVL into liquid alkenes in the molecular weight range appropriate for transportation fuels.^[10] However, in heterogeneous catalysis processes, the operating temperatures and pressures are as high as 370–420 K and 10–30 bar, respectively.^[11] In some cases, molecular H₂ is a critical feedstock that accounts for a large portion of working capital in the heterogeneous catalytic hydrodeoxygenation of LA. In some locations, hydrogen needs to be transported in, making the cost of hydrogen even more expensive than the biomass feedstock itself.^[12]

In this respect, electrocatalytic hydrogenation (ECH)^[13] offers an effective and sustainable way to store renewable electricity in high chemical energy density compounds through the reduction of oxygen-rich, biomass-derived compounds by using hydrogen generated in situ at the surface of metal electrodes. This process does not require an external supply of molecular hydrogen, and thus, eliminates the need for high temperatures and pressures to ensure good mass transport within the solid–liquid–gas interface. For example, ECH of lactic acid on a Ru/C catalyst in a one-compartment electrolysis cell has been studied; however, it led to an 80% yield of lactaldehyde and only minor amounts of 1,2-propandiol with a very low Faradaic efficiency (10^{−2}–10^{−5}%).^[14] Most recently, Nilges et al. demonstrated the feasibility of the ECH of LA to give VA by using a standard H-type electrolysis cell.^[15]

Current research efforts have been focused on the storage of renewable electrical energy as gaseous fuels,^[16] such as H₂ and methane, through electrolysis processes, that is, the wind-to-hydrogen project by the US DOE,^[17] and the Windgas project by Greenpeace Energy.^[18] From energy-conservation, economic, and sustainable-chemistry perspectives, it is more attractive to explore electrocatalytic processes to directly store renewable electricity in high-energy-density liquid fuels by using abundant, renewable, lignocellulosic biomass feedstock, especially when considering that robust infrastructure for the transportation of liquid fuels already exists. As shown in Table 1, the energy densities of gVL (2.65 MJ mol^{−1}) and VA (2.84 MJ mol^{−1}), which are the two main LA ECH products, are higher than that of LA (2.42 MJ mol^{−1}); this indicates that LA can serve as a starting compound for renewable electricity storage.

This work involves an investigation into an ECH route based on a non-precious-metal Pb electrode that can selectively convert LA into biofuel precursors (VA or gVL) of higher energy density with low electricity input. We demonstrate the ECH of

Table 1. Physical properties of valeric biofuel-related compounds.

Compound	b.p. ^[a] [°C]	m.p. ^[a] [°C]	State at STP ^[b]	Molar mass [g mol ^{−1}]	Density [kg L ^{−1}]	Solubility limit [g L ^{−1}]	Energy density		
							[MJ mol ^{−1}]	[MJ L ^{−1}]	[MJ kg ^{−1}]
VA	186	−35	liquid	102.1	0.93	40 ^[c]	2.84	25.9	27.8
gVL	208	−31	liquid	100.1	1.05	≥ 100 ^[d]	2.65	27.8	26.5
LA	246	34	solid	116.2	1.15	miscible ^[e]	2.42	24.0	20.8

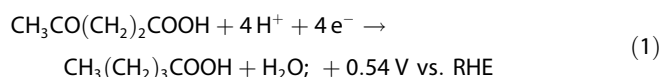
[a] b.p. = boiling point; m.p. = melting point. [b] STP: standard conditions for temperature (298.15 K) and pressure (100 kPa). [c] Data from the Material Safety Data Sheet (MSDS) by Sigma-Aldrich. [d] Data from <http://en.wikipedia.org/wiki/Gamma-Valerolactone>. [e] Data from MSDS by Acros Organics.

LA to give VA with a high selectivity (95%) at a high Faradaic efficiency (86.5%), low electricity consumption (EC; 1.5 kWh L_{VA}^{−1}), and a high electricity storage efficiency (ESE) of 70.8% in a single electrocatalytic (flow) cell reactor. A very high yield of VA (>90%) and good catalyst durability were also achieved. In addition, we discovered that the applied potentials and electrolyte pH could be used to regulate the selectivity of LA ECH products: lower overpotential or higher pH electrolyte favored the formation of gVL, whereas a higher overpotential or lower pH electrolyte facilitated the formation of VA. We also thoroughly investigated the molecular structure effects on the electrocatalytic reduction of hydroxyl, ketone, and aldehyde groups of biomass-relevant compounds in terms of reactivity, selectivity, and reaction pathway. Our work may open up an alternative way to efficiently store renewable electrical energy in biofuel-related compounds by using a biomass-derived intermediate feedstock.

Results and Discussion

Thermodynamics and kinetics of the ECH reaction

From a thermodynamic point of view, the reversible potential of the hydrogenation of LA to VA is around 500 mV more positive than that of the hydrogen evolution reaction (HER) across the entire pH range, as shown in Figure 1. This indicates that, since LA reduction involves H₂O and H⁺, the reversible potential varies in accordance with the pH of the electrolyte. In addition, the boundary region where the stable acid (LA and VA) and salt (levulinate and valerate) forms exist in the electrolyte is also shown; this is dependent on the electrolyte pH. At pH 0 at room temperature, the thermodynamically stable forms are LA and VA ([CH₃CO(CH₂)₂COOH]/[CH₃CO(CH₂)₂COO[−]] = 42 000; [CH₃(CH₂)₃COOH]/[CH₃(CH₂)₃COO[−]] = 66 000). The ECH of CH₃CO(CH₂)₂COOH to CH₃(CH₂)₃COOH in aqueous solution is given in Equation (1) with respect to the reversible hydrogen electrode (RHE):



At a pH value of 7.5, the salt-to-acid ratios are [CH₃CO(CH₂)₂COO[−]]/[CH₃CO(CH₂)₂COOH] = 2400 as well as [CH₃(CH₂)₃COO[−]]/[CH₃(CH₂)₃COOH] = 1500; therefore, valerate,

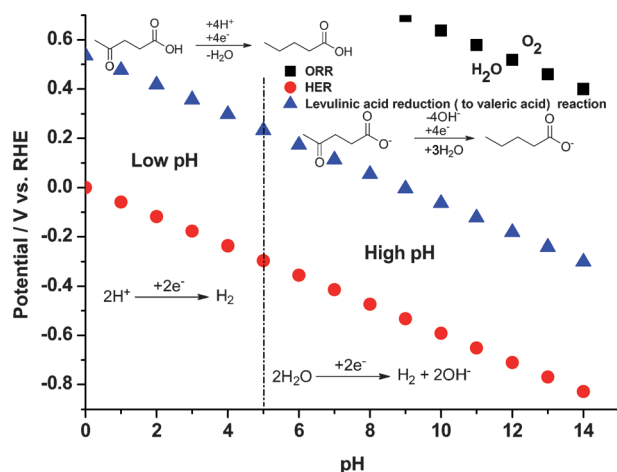
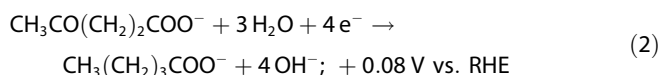


Figure 1. Theoretical potential for the oxygen reduction reaction (ORR), the HER, and the electrochemical hydrogenation of LA to VA as a function of pH.

$\text{CH}_3(\text{CH}_2)_3\text{COO}^-$, is predominantly produced from levulinate, $\text{CH}_3\text{CO}(\text{CH}_2)_2\text{COO}^-$, as shown in Equation (2):



As shown in Figure 1, the ECH of LA to VA is a thermodynamically favorable reaction compared with the HER. However, kinetically the HER proceeds faster on the metal electrode compared with the ECH of LA, and therefore, the actual electrolysis potentials for ECH of LA and HER are very similar. Previous works have provided the mechanism of the HER,^[19] which proceeds through the steps shown in Equations (3)–(7):

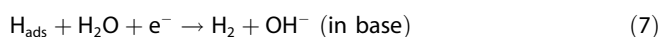
Volmer step:



Tafel step:



Heyrovsky step:



The adsorbed hydrogen generated from the Volmer step serves as the hydrogen source for subsequent ECH steps. The Tafel and Heyrovsky steps facilitate the HER, which are unwanted side reactions that reduce the surface adsorbed hydrogen density and consume the applied electricity (decrease the Faradaic efficiency). Since the electrochemical steps in Equations (3)–(7) govern the availability of adsorbed hydrogen, it is expected that the ECH selectivity and reaction rate will be af-

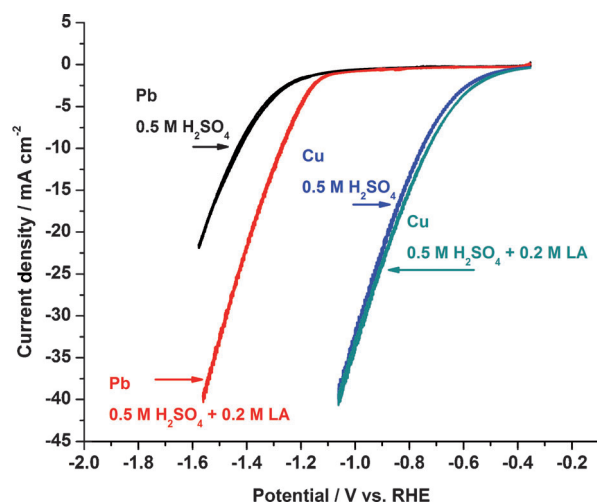


Figure 2. CVs of the ECH of LA on Pb and Cu in an acidic electrolyte (pH 0) at a scan rate of 50 mV s^{-1} , room temperature, and ambient pressure.

ected by the applied potential, the electrolyte pH, and the metal catalyst.

Figure 2 shows cyclic voltammograms (CVs) of the ECH of LA on pretreated Pb and Cu electrodes. The cyclic voltammetry scan was performed in a 0.5 M solution of H_2SO_4 with or without 0.2 M LA at a scan rate of 50 mV s^{-1} . From the CVs of the Pb electrode with or without the addition of 0.2 M LA, it is clear that the onset potential is over 200 mV more positive and the cathodic current is significantly greater with 0.2 M LA than that without LA. In sharp contrast, the HER in $0.5\text{ M H}_2\text{SO}_4$ on Cu occurs at -0.4 V , which is 700 mV more positive compared with -1.1 V for Pb. However, in the absence and presence of 0.2 M LA, the cathodic current density remains almost the same on the Cu electrode, indicating that the adsorption of LA or charge transfer due to the ECH of LA is suppressed by the very fast HER on Cu. The product analysis shown in Table 2 (entry 8) confirms that the conversion of LA is zero on the Cu electrode, indicating that electrons transferred are all attributed to the HER. According to the Faraday Law,^[20] the net current flow during the electrochemical reaction can be proportionally attributed to the amount of LA converted in the given time period. Valuable information about the extent of the ECH of LA accompanied by the HER is provided by cyclic voltammetry experiments. However, product analysis needs to be carried out under different reaction conditions to investigate the extent of the LA ECH reaction and to further elucidate reaction pathways.

Potential/pH-regulated selective ECH of LA to VA and gVL on a Pb electrode in a half-cell (batch) reactor

Selective ECH of LA was conducted in a half-cell (batch) reactor with 55 mL of electrolyte. Chronoamperometry (CA) was carried out under different applied voltages for 1 h . As summarized in Figure 3 and Table 2, the selective production of gVL and VA on a Pb electrode was governed by the extent of polarization of the Pb electrode, which could be controlled by the

Table 2. ECH of LA in half-cell (batch) and single electrocatalytic (flow) cell reactors.^[a]

Entry	Reactor configuration	Catalyst	Solvent	pH	<i>E</i> [V vs. RHE]	Reaction time [h]	EC [kWh L _{VA} ^{−1}]	Selectivity ^[b] [%]	Faradaic efficiency ^[c] [%]	Conversion [%]
1	half-cell	Pb	H ₂ O/H ₂ SO ₄	0	−1.5	1	1.9	97.0 (to VA)	78.3	20.3
2	half-cell	Pb	H ₂ O/H ₂ SO ₄	0	−1.3	1	1.6	94.1 (to VA)	83.8	6.7
3	half-cell	Pb	H ₂ O/H ₂ SO ₄	0	−1.1	1	4.3	81.5 (to VA)	27.9	1.2
4	half-cell	Pb	H ₂ O/H ₂ SO ₄	0	−1.3	2	1.6	94.5 (to VA)	84.2	12.7
5	flow cell	Pb	H ₂ O/H ₂ SO ₄	0	−1.3	2	1.5	95.0 (to VA)	86.5	18.6
6	half-cell	Pb	H ₂ O/Buffer	7.5	−1.3	2	10.8 (to gVL)	100 (to gVL)	6.2	1.3
7	flow cell	Pb	H ₂ O/Buffer	7.5	−1.3	2	4.0 (to gVL)	100 (to gVL)	18.2	4.5
8	half-cell	Cu	H ₂ O/H ₂ SO ₄	0	−0.8	1	∞	0 ^[d]	0 ^[e]	0

[a] Reaction conditions: ambient pressure and room temperature. [b] Selectivity of the product in liquid electrolyte. [c] Faradaic efficiency takes account of the sum of electrons transferred to both VA and gVL during ECH of LA. [d] No reduction products are detected in the liquid phase. [e] All electrons transferred are attributed to HER; the Faradaic efficiency to products in liquid electrolyte is zero.

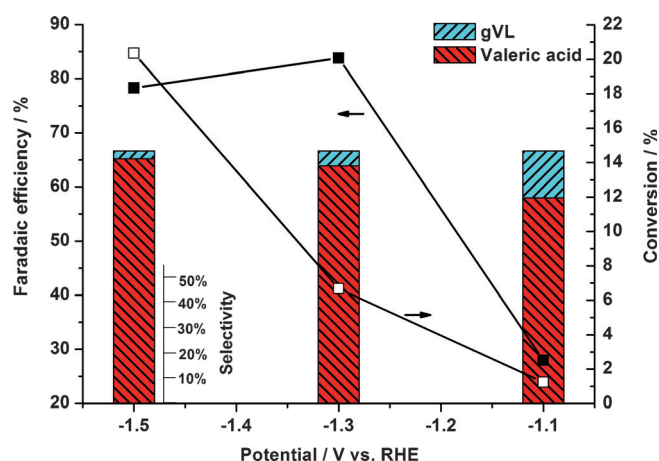


Figure 3. Selective ECH of LA on a Pb electrode in a half-cell (batch) reactor under different applied potentials; the Faradaic efficiency is related to the liquid products (VA + gVL); reaction conditions: 0.5 M H₂SO₄ + 0.2 M LA, room temperature, ambient pressure, 1 h.

applied potential. At −1.1 V, which is close to the onset potential of LA ECH on the Pb electrode, 81.5% selectivity to VA (18.5% to gVL) was observed at a Faradaic efficiency of 27.9% and LA conversion of 1.2%. When the applied voltage decreased to −1.3 V, the VA selectivity increased to 94.1% (5.9% to gVL), while the ECH Faradaic efficiency and LA conversion increased to 83.8 and 6.7%, respectively. When the applied potential further decreased to −1.5 V, the selectivity of VA increased to 97.0% and the conversion of LA jumped to 20.3% after 1 h reaction, while the Faradaic efficiency slightly dropped to 78.3%. The results demonstrate that the ECH of LA (CH₃CO(CH₂)₂COOH) might involve a serial four-electron pathway through the reaction intermediate 4-hydroxypentanoic acid (CH₃COH(CH₂)₂COOH_{ads}), the presence of which was proposed by Dumesic's group.^[9a] The adsorbed 4-hydroxypentanoic acid can be further reduced to VA (CH₃(CH₂)₃COOH) or desorbed into the bulk electrolyte to form gVL. The more negative the potential applied, the higher the selectivity of VA that can be achieved with less gVL detected.

The variation of Faradaic efficiency at different applied potential observed in Figure 3 is consistent with the CV and Tafel

plot (Figure 2 and Figure S1 in the Supporting Information). Within the voltage range close to the onset potential at which the degree of Pb polarization is insufficient for LA reduction, the ECH of LA proceeds slowly. Thus, only a slight difference in the cathodic current density was observed with and without LA was observed, leading to a lower Faradaic efficiency (27.9%). With more negative applied voltage potentials, the availability of surface H_{ads} atoms increases. The ECH of LA accelerates, as illustrated in Figure 2, when the slope of the CV curve in the presence of LA becomes steeper than the blank electrolyte as the applied potential becomes more negative. However, the more negative the applied potential is, the unwanted HER step is more competitive, proceeding through Tafel or Heyrovsky steps [Eqs. (5) and (6)]. This is supported by the increasing Tafel slope due to the mass transport issue arising from hydrogen gas bubbles generated on the Pb electrode surface as the applied potential becomes higher than −1.4 V, as shown in Figure S1 b in the Supporting Information. Therefore, the measured Faradaic efficiency reaches a maximum at −1.3 V (83.8%) and decreases to 78.3% at −1.5 V.

To evaluate the energy efficiency of the LA ECH reaction, the EC is defined in Equation (8):

$$EC = \frac{\text{electrical energy input}}{\text{unit product}} = \frac{EIt/1000}{\text{unit product}} \quad (8)$$

in which *E* is the applied potential (in V vs. RHE); *I* is the current (in A); *t* is the reaction time (in h); and EC is given in kWh mol_{product}^{−1} or kWh L_{product}^{−1}. A lower EC value means that the production of the target product (e.g., VA) requires a smaller amount of electrical energy input. The introduction of EC combines the Faradaic efficiency, the overpotential, and product yield (conversion × selectivity) to quantify the energy efficiency of the ECH process. Based on the ECH reaction carried out in the half-cell (batch) reactor, the lowest EC of 1.6 kWh L_{VA}^{−1} was achieved at −1.3 V, as shown in Table 2 and Figure S2 in the Supporting Information. Thus, with an electricity input of 1.6 kWh, 1 L of VA with a higher energy density (25.9 MJ L^{−1}, compared with LA of 24.0 MJ L^{−1}) can be produced. Based on the current industrial electricity rate of \$0.068 kWh^{−1} in the US, including demand charges, all other

end-use costs and state and local taxes,^[21] the cost of the electricity is only \$0.42 for the production of 1 gallon of VA from LA. In addition, the conversion of LA to VA results in removal of the oxygen content in the biomass-derived oxygenate compound. Less-oxygen-containing VA is an important biofuel precursor for the next step of upgrading to valeric biofuels.^[9b]

The dependence of pH on the selectivity for ECH of LA on the Pb electrode was also investigated in a half-cell (batch) reactor with 0.2 M LA + 0.5 M H₂SO₄ (pH 0) or K₂HPO₄/KH₂PO₄ buffer solution (pH 7.5) as the electrolyte. Figure 4 presents the CV curves of ECH of LA as a function of pH. The observed cur-

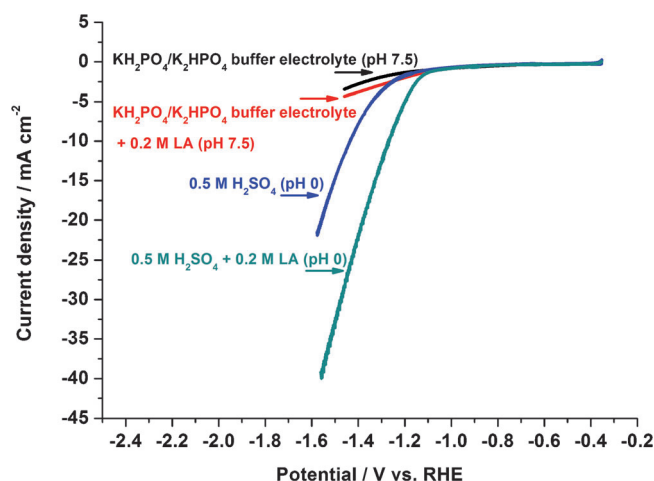


Figure 4. CVs of ECH of LA on a Pb electrode as a function of pH at 50 mV s⁻¹, room temperature, and ambient pressure.

rent density in neutral electrolyte is generally much lower than that in acid medium, regardless of the addition of LA. This is probably due to the different kinetics and pathways for the ECH reactions in acid and neutral environments. Thus, the hydrogenation rate and selectivity would be expected to be a function of the electrolyte pH. Table 2 (entries 4 and 6) shows that the ketone group of LA can be fully reduced to -CH₂- by a four-electron-transfer reduction to VA in low pH electrolyte (high H⁺ concentration), whereas it is partially reduced to -OH in neutral electrolyte and involves only two-electron-transfer reduction. A selectivity of 100% to gVL at an LA conversion of 4.8% was achieved, although the EC in neutral electrolyte (10.8 kWh L_{gVL}⁻¹) is much higher than that in acidic electrolyte (1.6 kWh L_{VA}⁻¹). The kinetic behavior of LA ECH on the Pb electrode in acid and neutral electrolytes was revealed by the analysis of Tafel plots. Figure S1 in the Supporting Information shows that both HER and ECH of LA proceed faster and require a lower overpotential to obtain a certain current density in the acidic electrolyte than those in the neutral solution. The number of electrons transferred in the acidic electrolyte with the presence of LA is twice of that in a blank 0.5 M solution of H₂SO₄, leading to a four-electron-transfer reaction that favors the production

of VA. In comparison, ECH of LA on a Pb electrode involves two-electron-transfer (the same as the HER) to generate gVL in a neutral environment. It can also be inferred from the Tafel slope investigation that the energy required for the reactants to adsorb on the Pb electrode at a lower pH is lower than that at higher pH, resulting in an increase in the production rate of H_{ads} atoms as well as molecular hydrogen. The higher coverage of H_{ads} atoms and LA on the Pb electrode in an acidic electrolyte could lower the energy barrier for complete reduction of the ketone group of LA to -CH₂- by a four-electron-transfer pathway. In the neutral electrolyte, both LA and monoatomic hydrogen adsorb weakly on the Pb electrode; therefore, only the partial reduction product gVL (by a two-electron-transfer pathway) was observed. (See the Supporting Information for a detailed discussion.)

Selective ECH of LA on a Pb electrode in a single electrocatalytic (flow) cell reactor

The ECH of LA was conducted in a custom-made single electrocatalytic (flow) cell reactor, as illustrated in Figure 5.^[22] During each run, 55 mL of 0.2 M LA in 0.5 M H₂SO₄ (pH 0) or KH₂PO₄/K₂HPO₄ buffer (pH 7.5) solution flowed in a closed looped through the cathode chamber by a peristaltic pump. Meanwhile, the electrolyte without LA was cycled into the anode chamber to remove O₂ generated during the oxygen evolution reaction (OER) on the Pt foil anode. The applied potential on the cathode was controlled at -1.3 V versus RHE by using a potentiostat (VersaSTAT MC, Princeton Applied Re-

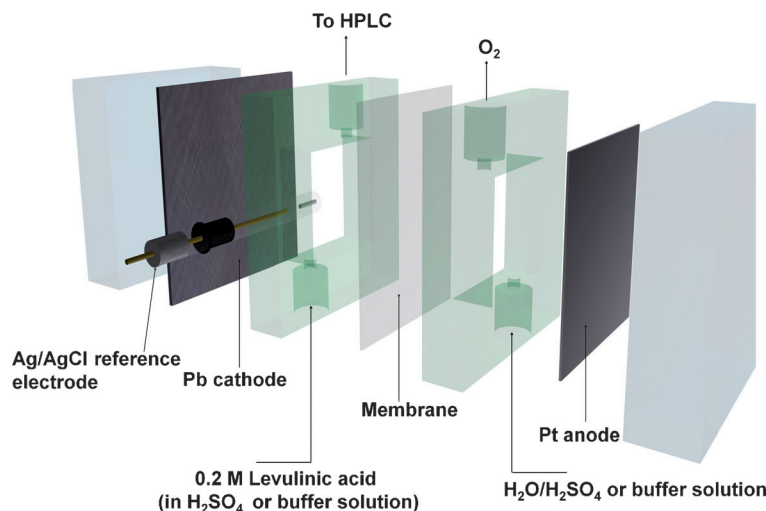


Figure 5. Schematic representation of a single electrocatalytic (flow) cell reactor.

search) for 2 h. In contrast to the half-cell (batch) reactor configuration, which is regarded to be a batch reactor, the single electrocatalytic (flow) cell reactor can be considered as a fixed-bed continuous flow reactor. Interestingly, we observed amazing consistency in the pH-dependent selectivity of the products between the single electrocatalytic (flow) cell and half-cell (batch) reactors, as shown in Table 2 (entries 4–7). At pH 0, the

selectivity for VA and gVL in the single electrocatalytic (flow) cell reactor is 95.0 and 5.0%, respectively; these values are in good agreement with the values achieved in a half-cell (batch) reactor: 94.5 and 5.5%. At pH 7.5, ECH of LA in both reactors yields 100% selectivity to gVL.

In addition, the ECH of LA conducted in the single electrocatalytic (flow) cell reactor demonstrates higher Faradaic efficiency and LA conversion than the half-cell (batch) reactor, as shown in Table 2 (entries 4–7) and Figure 6. In neutral elec-

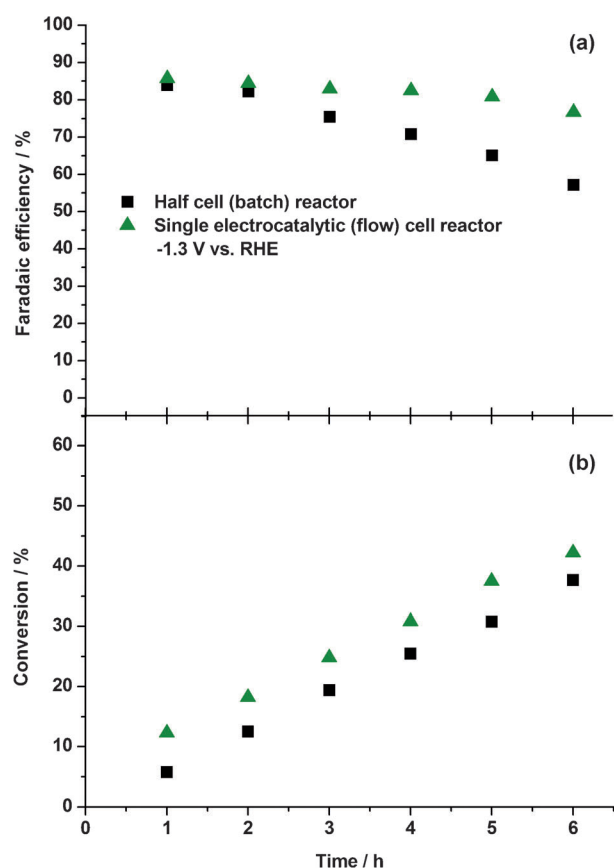


Figure 6. (a) Conversion and (b) Faradaic efficiency versus time at an applied potential of -1.3 V versus RHE for a half-cell (batch) reactor and a proton exchange membrane (PEM)-based single electrocatalytic (flow) cell reactor with a Pb electrode. Reaction conditions: 0.2 M LA + 0.5 M H_2SO_4 , room temperature, and ambient pressure. The Faradaic efficiency is related to the liquid products (VA + gVL).

trolyte (pH 7.5), the ECH of LA performed in the single electrocatalytic (flow) cell reactor gives a higher Faradaic efficiency of 18.2% and a conversion of 4.5%, with respect to 6.2 and 1.3%, respectively, obtained in a half-cell (batch) reactor under the same reaction conditions. Table 2 (entries 6 and 7) shows the specific EC for the ECH process evaluated in both reactors at pH 7.5. It only requires 4.0 kWh to produce 1 L gVL in the single electrocatalytic (flow) cell reactor, which is less than half of the electrical energy input of 10.8 kWh for the production of 1 L gVL obtained in the half-cell (batch) reactor. On the other hand, in acidic electrolyte, during the 6 h reaction, the conver-

sion of LA achieved in a single electrocatalytic (flow) cell reactor at -1.3 V is also generally 7% higher than that in the half-cell (batch) reactor under identical reaction conditions. Notably, the Faradaic efficiency of the half-cell (batch) reactor decreases much faster than that in the single electrocatalytic (flow) cell reactor. After the 6 h reaction, the Faradaic efficiency dropped to only 57.2% in the half-cell (batch) reactor, while a higher Faradaic efficiency of 76.7% was still maintained in the single electrocatalytic (flow) cell reactor. Better performance of the single electrocatalytic (flow) cell reactor versus the half-cell (batch) reactor could be attributed to the custom design and optimized operation conditions in the single electrocatalytic (flow) reactor. The large electrode area (6.5 cm^2) and the small cathode chamber volume (12 mL) along with the fast flow rate of 30 sccm were optimized to ensure a sufficient supply of LA to the Pb electrode surface, while avoiding the mass transport issue caused by hydrogen gas bubbles striking the Pb electrode. When ECH of LA is conducted in an acidic environment, in which the reaction proceeds faster than that in neutral electrolyte, as the reaction time was extended to more than 2 h, the HER started to dominate because depletion of LA generates more hydrogen bubbles on the Pb electrode surface. Interference from gas bubbles, preventing a fresh supply of LA to the catalyst surface, is much more serious in the half-cell (batch) reactor, even though the stirring rate has been optimized to minimize such mass transport issues.

To investigate the durability of the Pb electrode in acidic solution, the ECH of LA performed in a PEM-based single electrocatalytic (flow) cell reactor was extended to 20 or 10 h at applied potentials of -1.3 and -1.5 V, respectively. Liquid reactor effluent was collected at certain time intervals and the reactant and product concentrations were analyzed by using an HPLC system. Figure 7 shows that, after continuous reaction for 20 or 10 h, the conversion of LA at -1.3 and -1.5 V can reach 91.1 and 96.8%, respectively. The reaction rate illustrated in Figure S3 in the Supporting Information shows that the ECH of LA at -1.5 V is faster than that at -1.3 V, confirming that a more negative potential can activate the hydrogenation of LA on the Pb electrode (see the Supporting Information for a detailed discussion). In addition, as the conversion of LA increases, the Faradaic efficiency is observed to decrease because the HER becomes more competitive as more LA is converted. However, Figure 8a and b demonstrates that the selectivities to VA and gVL are almost constant at 93.3 and 6.7%, respectively, at -1.3 V after 20 h, and at 96.9 and 3.1%, respectively, at -1.5 V after 10 h reaction. Inductively coupled plasma atomic emission spectroscopy (ICP-AES) analysis indicated that no measurable quantities of Pb ions (<2 ppm) were detected in the liquid reactor effluent after reaction for 20 and 10 h. In addition, no clear difference was observed in the CV curves carried out in blank 0.5 M H_2SO_4 before and after prolonged reaction (Figure S4 in the Supporting Information). Therefore, these results suggest good stability of the Pb electrode and that no detectable Pb leaching occurred during the extended reaction study in low-pH electrolyte (pH 0) at negative potentials (<-1.3 V).

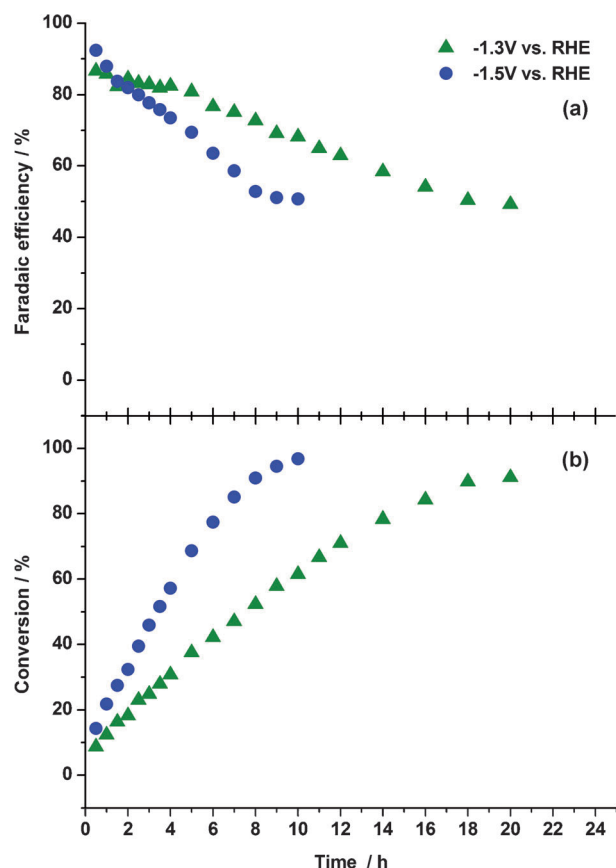


Figure 7. (a) Conversion and (b) Faradaic efficiency of LA ECH versus time at applied potentials of -1.3 and -1.5 V versus RHE on a Pb electrode in a PEM-based single electrocatalytic (flow) cell reactor. Reaction conditions: 0.2 M LA + 0.5 M H_2SO_4 , room temperature, and ambient pressure. The Faradaic efficiency is related to the liquid products (VA + gVL).

Significantly, it is exciting to observe that the yield of VA could reach up to 84.0 and 93.4% at -1.3 and -1.5 V, respectively, as shown in Figure 9. Meanwhile, EC analysis shows that even though the ECH of LA proceeds faster and the yield of VA is higher at -1.5 V than that at -1.3 V, the EC at -1.5 V is greater than that at -1.3 V, mainly due to the 200 mV higher overpotential required to accelerate the reaction. Thus, there is a trade-off between the product yield, reaction rate, and the EC; all of which need to be taken into consideration during practical ECH operation. The high yield of VA achieved in the PEM-based single electrocatalytic (flow) cell reactor will significantly reduce the cost of subsequent energy-intensive processes for the separation of target products. Additionally, it has been reported that LA can be produced by a simple and cost-efficient acid-catalyzed hydrolysis of waste cellulosic materials by H_2SO_4 .^[4,6b,23] However, the presence of H_2SO_4 will dramatically deactivate the catalysts employed to heterogeneously reduce LA.^[24] Some energy-intensive processes, such as solvent extraction combined with distillation, are required to separate LA from H_2SO_4 before the catalytic hydrogenation of LA; thus making the overall process complicated and costly.^[8b] The introduction of a single electrocatalytic (flow) cell reactor presented herein offers a feasible strategy to directly use outlet

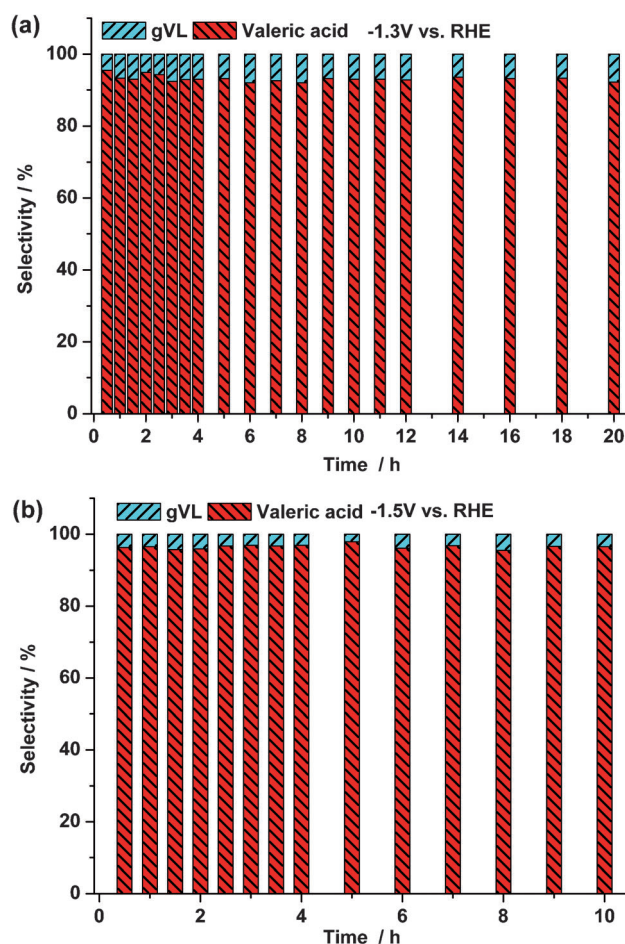


Figure 8. Selectivity of LA ECH versus time at applied potentials of a) -1.3 and b) -1.5 V versus RHE on a Pb electrode in a PEM-based single electrocatalytic (flow) cell reactor. Reaction conditions: 0.2 M LA + 0.5 M H_2SO_4 , room temperature, and ambient pressure. The Faradaic efficiency is related to the liquid products (VA + gVL).

streams of the cellulosic hydrolysis process (LA + aqueous H_2SO_4); this could reduce the capital costs required to upgrade LA to a biofuel. Another big issue is the need for molecular hydrogen in the chemical catalytic reduction of LA. It is claimed that the cost of hydrogen in some locations is often higher than the biomass itself.^[25] The ECH of LA conducted in a single electrocatalytic (flow) cell reactor does not require an external molecular hydrogen source and uses an inexpensive non-precious metal Pb electrode. Taken together, the single electrocatalytic (flow) cell reactor is particularly suited for sustainable processing of biorenewable compounds under continuous operation and the whole process is viable for scaleup.

Additionally, the single electrolysis (flow) cell reactor provides a new strategy to store renewable electricity produced by solar cells and wind power into liquid fuel compounds by taking advantage of the chemical potential differences between LA (2.42 MJ mol^{-1}) and VA (2.84 MJ mol^{-1}) or gVL (2.65 MJ mol^{-1}) to capture electrical energy during off-peak hours. Off-peak electricity can be used to efficiently convert LA into VA or gVL, which can be further upgraded to hydrocarbon fuels, such as octane.^[9b,10,26] The efficiency of converting ap-

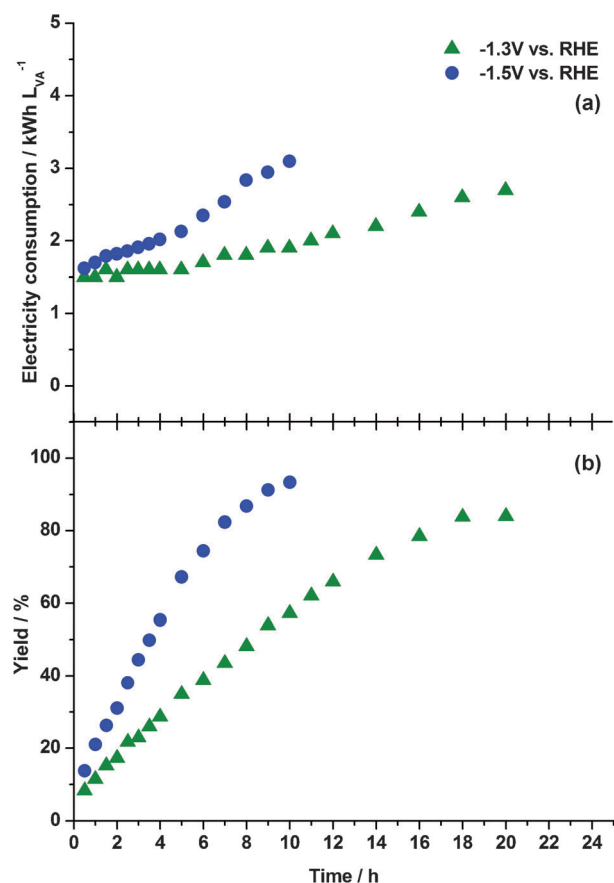


Figure 9. (a) Electricity consumption (EC) and (b) yield of VA versus time at applied potentials of -1.3 and -1.5 V versus RHE on a Pb electrode in a PEM-based single electrocatalytic (flow) cell reactor. Reaction conditions: 0.2 M LA + 0.5 M H_2SO_4 , room temperature, and ambient pressure. The Faradaic efficiency is related to the liquid products (VA + gVL).

plied electricity into stored chemical energy in a specific product (VA or gVL) for ECH of LA is measured by ESE [Eq. (9)]:

$$\text{ESE} = \frac{\text{mol (specific identified product)} \times \Delta_c H^\circ_{\text{LA} \rightarrow \text{VA or gVL}}}{EIt/1000} \quad (9)$$

in which E is the applied potential (in V vs. RHE), I is the current (in A), t is the reaction time (in h), and $\Delta_c H^\circ_{\text{LA} \rightarrow \text{VA or gVL}}$ is the difference in the standard enthalpy change of combustion between LA and VA or gVL (in kJ mol^{-1}). A higher ESE means that more electrical energy is stored in more energetic fuel compounds.

Figure 10 shows the ESE of selective ECH of LA to VA or gVL in a single electrocatalytic (flow) cell reactor on a Pb electrode in aqueous solution with different pH values at an applied potential of -1.3 V. At pH 0, 70.8% of the electrical energy is directly stored in VA (with 95% selectivity), whereas 16.7% of electrical energy is stored in gVL (with 100% selectivity) at pH 7.5. (A detailed calculation of ESE is tabulated in Table S1 in the Supporting Information.) The ESE obtained at pH 0 is significantly greater than the ESE achieved at pH 7.5. This result is within our expectations because the relative reaction rate ratio of ECH to HER is greater in an acidic electrolyte than that in

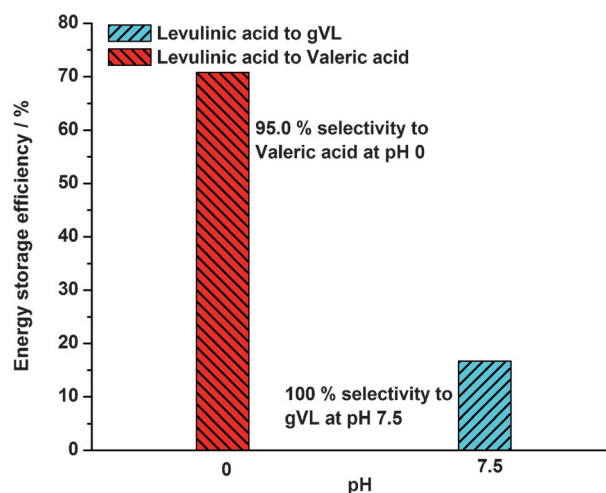


Figure 10. ESE of the selective ECH of LA to VA or gVL on a Pb electrode in a single electrocatalytic (flow) cell reactor at different pH values. Reaction conditions: 0.2 M LA, room temperature, ambient pressure, -1.3 V versus RHE, 2 h.

a neutral electrolyte and the current density generated at pH 0 is about 40% higher than that at pH 7.5 in the single electrocatalytic (flow) cell reactor.

Comparison of current electricity storage techniques with electricity storage in biofuels

Electrical energy storage techniques are methods of converting renewable electrical energy, that is, photovoltaic and wind power, during off-peak hours into other forms of energy for later use. Current electrical energy storage techniques include PSH, CAES, batteries, flywheels, and electrolysis of water to hydrogen (electro-hydrogen) for fuel cells, as well as chemical catalytic hydrogenation, and so forth.^[2] PSH has a high efficiency (70–85%) and long storage duration; however, the large amount of land required for the construction of a hydro-dam and reservoir can increase construction costs and lower overall feasibility. CAES also has a high efficiency (70–89%), long storage duration, and has attracted extensive attention recently, but it can only be constructed in areas with favorable geography because it needs to be used in conjunction with a gas turbine plant. Batteries are primarily for short-term storage and have more limited energy storage capacities, that is, Li ion batteries have an effective practical energy density of only 0.35 kWh kg^{-1} , which is approximately 20% that of gasoline.^[27]

Production of H_2 through electrolysis of water (electro-hydrogen) for H_2 -proton exchange membrane fuel cells (PEMFCs) is another sustainable energy cycle option.^[28] Low-temperature H_2 -based PEMFCs can directly convert chemical energy stored in H_2 into electricity without limitation of the Carnot cycle.^[29] However, a high loading of noble metals (i.e., >0.6 mg of Pt per electrode) is required in PEMFCs to facilitate the sluggish oxygen reduction reaction (ORR) at the cathode; this is a long-standing scientific issue, which dramatically decreases the energy conversion efficiency.^[30] Although the theoretical ther-

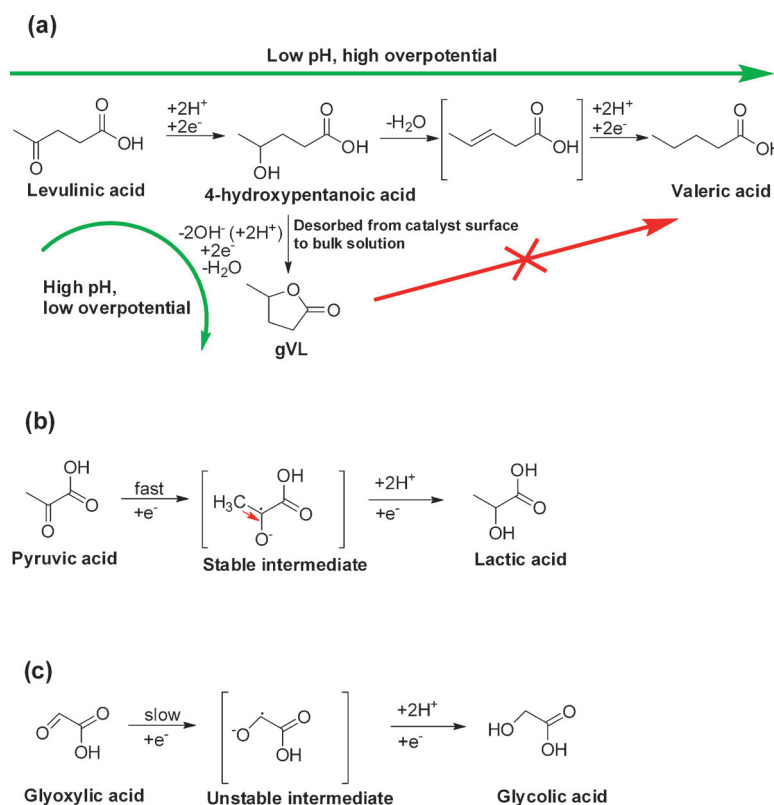
modynamic efficiency of a H_2 fuel cell is 83% under standard conditions, the operating voltage must be significantly decreased for a high power output, that is, 0.65 V. Unfortunately, the resulting thermoefficiency is only about 44%. Considering the electrical current efficiency for H_2 production in a PEM-based electrolysis cell is around 70%, the overall energy efficiency of fuel cell + electrolysis cell based on the hydrogen cycle is only 30%.^[2] This does not even include the energy loss from fuel cells to mechanic motors (to wheels). In addition, both fuel (consumption of H_2) and electrolysis (generation of H_2) cells have to employ very expensive precious metals, such as Pt (for the ORR)^[30a] and Ir (for the OER).^[31] In an acidic-electrolyte environment, the durability of both the catalyst (even noble metals) and membrane (even C–F backbone polymers) still needs improvement to achieve widespread application of PEMFCs in automobiles.^[32] Furthermore, storage and transportation of H_2 have encountered significant challenges compared with well-established liquid fuel pipeline systems. In addition, a significant disadvantage of using electro-hydrogen for conventional catalytic hydrogenation of biomass compounds to biofuels is capture of gaseous hydrogen from water electrolysis processes for high temperature and pressure hydrogenation of biomass feedstocks. This will increase capital and operation costs; thus making it economically inferior and technically difficult to scale up. The safety issues associated with pressurized hydrogen will also arise from this biofuel upgrading route.

The direct storage of electrical energy in high-energy-density liquid fuels using a single electrocatalytic (flow) cell reactor presented herein shows singular characteristics that are superior to the electricity storage systems mentioned above. A main advantage is that the electrical energy can be stored directly in liquid fuels that are suitable for blending. For transportation (autos, ships, and airplanes) applications, the most desirable energy carriers are long-chain hydrocarbon fuels, such as gasoline, diesel, and kerosene, due to their unparalleled high energy density.^[3b] For example, the theoretical energy density of gasoline is very high: 13 kWh kg^{-1} (46.8 MJ kg^{-1} , 9.14 kWh L^{-1}). Even considering its tank-to-wheel efficiency (including Carnot efficiency) of 12.6%, gasoline remains a highly effective energy density of 1.7 kWh kg^{-1} .^[27] Moreover, robust infrastructures already exist for storage and transportation of liquid fuels.

Therefore, although active R&D activities are still underway to achieve higher efficiency of the current electrical energy storage techniques, seeking new electrochemistry-based energy storage methods should be simultaneously promoted, to diversify and secure our energy future. The electrobiofuel technique presented for converting biomass-derived feedstock to biofuel-related compounds will provide a promising and sustainable way to store renewable electricity and will have potential to alleviate our long-time addiction to non-renewable petroleum sources.

Reaction pathway and molecular structure effects on ECH of oxygenates containing ketone or aldehyde groups

Based on the results obtained from the half-cell (batch) and single electrocatalytic (flow) reactors, the reaction pathway for the ECH of LA is proposed in Scheme 1a. As discussed before, the ketone group in LA is able to be selectively reduced to $-OH$ (two-electron transfer) or fully reduced to $-CH_2-$ (four-electron transfer): Lower overpotentials favor the production



Scheme 1. Proposed reaction pathway for the ECH of LA to form gVL (a), pyruvic acid (b), and glyoxylic acid (c) in acidic electrolyte on Pb.

of gVL (18.5% selectivity to gVL at -1.1 V), whereas higher overpotentials facilitate the formation of VA (97% selectivity to VA at -1.5 V). At low applied potentials, both the ketone group of LA and monoatomic hydrogen adsorb weakly on the Pb electrode, resulting in the slower reaction rate and lower current density observed (Figure 11). According to the pro-

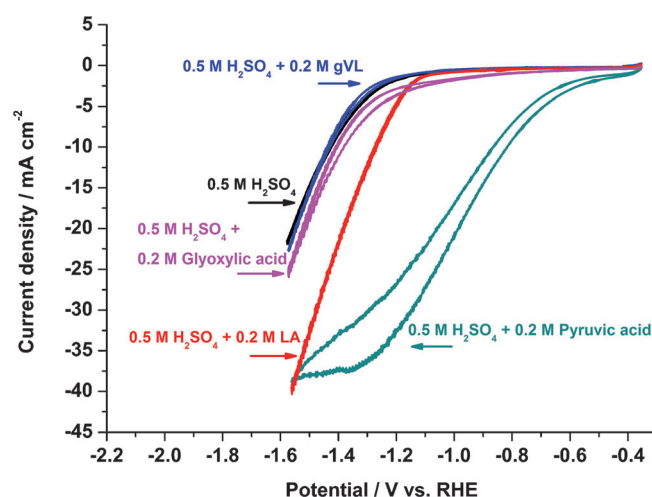


Figure 11. CVs of the ECH of biomass compounds containing ketone or aldehyde groups on a Pb electrode in acidic electrolyte at a scan rate of 50 mV s^{-1} , room temperature, and ambient pressure.

posed sequential mechanism for ECH of LA on a Pb electrode (Scheme 1 a), the reaction intermediate (4-hydroxypentanoic acid) is more weakly adsorbed on the Pb electrode surface than LA. This can be supported by the experiment using the esterification intermediate gVL as a feedstock, for which the CV curve of the ECH of 0.2 M gVL on Pb in 0.5 M H_2SO_4 does not show any difference compared with the blank CV curve recorded in 0.5 M H_2SO_4 electrolyte (Figure 11). The product anal-

potential, a more negatively polarized Pb electrode will perhaps not only facilitate the interaction of the C=O (ketone) group of LA with the Pb electrode surface, but also increase the concentration of surface H_{ads} atoms. Thus, a more negative potential could accelerate the hydrogenation of the C=O (ketone) group of LA to $-\text{CH}_2-$ with less desorbed gVL.

It has also been demonstrated that the pH value can be used to control the final product distribution. Selectivities of 95% to VA in acidic electrolyte (pH 0) and 100% to gVL in neutral electrolyte (pH 7) were obtained (Scheme 1 a). The effect of electrolyte pH on product selectivity was revealed by the Tafel plot investigation (Figure S1 in the Supporting Information), which showed that four-electron transfer was involved in the ECH of LA in acidic electrolyte, resulting in the formation of VA, whereas only two-electron transfer was observed in neutral electrolyte (pH 7.5), leading to the production of gVL.

To gain insight into structural effects on C=O reduction pathways, pyruvic acid and glyoxylic acid, which contain ketone or aldehyde groups, were also studied. Figure 11 depicts the half-cell CVs of the ECH of these oxygenates on Pb in an acidic electrolyte. A cyclic voltammetry scan in 0.2 M pyruvic acid + 0.5 M H_2SO_4 gave a 700 mV more positive onset potential and significantly greater current density than that conducted in 0.2 M LA electrolyte; this indicates Pb has a higher electrocatalytic activity towards the ECH of pyruvic acid than that of LA. In sharp contrast, with 0.2 M glyoxylic + 0.5 M H_2SO_4 , the ECH reaction rate was much slower on Pb than that with 0.2 M LA, as evidenced by the smaller current density observed in the CV curves.

It is interesting to observe that the ketone groups in pyruvic and glyoxylic acid can only be reduced to $-\text{OH}$ through a two-electron-transfer reaction compared with the ECH of LA on Pb in an acidic electrolyte, resulting in 100% selectivity to lactic acid and glycolic acid, respectively (Table 3). However, 89.6% conversion of pyruvic acid after 4 h ECH reaction is much higher than the conversion of both LA and glyoxylic acid, which are only 51.3 and 1.6% respectively.

This also agrees well with the cyclic voltammetry experiment, in which the ECH of pyruvic acid exhibited the greatest current density. The EC value for the target product, given by the yield, Faradaic efficiency, and applied potential, determines the specific energy consumption. As expected, the EC value for the conversion of pyruvic acid into lactic acid ($0.14 \text{ kWh mol}_{\text{lactic acid}}^{-1}$) is lower than both values for VA (from LA reduction) and glycolic acid (from glyoxylic acid reduction), the EC values of which are $0.29 \text{ kWh mol}_{\text{VA}}^{-1}$ and $3.23 \text{ kWh mol}_{\text{glycolic acid}}^{-1}$, respectively, as shown in Table 3 and Figure S5 in the Supporting Information. These results indicate that the final products may be influenced by the molecular structure of the oxygenated compounds. As illustrated in

Table 3. ECH of biomass compounds containing ketone or aldehyde groups in a half-cell (batch) reactor on Pb (pH 0).^[a]

Biomass compound	EC [kWh mol^{-1}]	Selectivity [%]	Faradaic efficiency ^[b] [%]	Conversion [%]
LA	0.29 (to VA)	95.0 (to VA)	57.1	51.3
gVL	∞	0 ^[c]	0 ^[d]	0
pyruvic acid	0.14 (to lactic acid)	100 (to lactic acid)	56.1	89.6
glyoxylic acid	3.23 (to glycolic acid)	100 (to glycolic acid)	2.5	1.6

[a] Reaction conditions: CA of -1.5 V vs. RHE was performed for 4 h in 0.5 M H_2SO_4 + 0.2 M biomass compound at room temperature. [b] Faradaic efficiency takes account the sum of electrons transferred during the ECH of LA to VA and gVL. [c] No products are detected in the liquid phase. [d] All electrons transferred are attributed to HER.

ysis shown in Table 3 further confirms that the conversion of gVL under identical conditions to the ECH of LA is 0, and 100% electron transfer is attributed to the HER. The results indicate that gVL is a relatively stable product under ECH conditions and further hydrogenation will not proceed, as long as it is produced and desorbed from the metal catalyst surface. Because the adsorption strength of 4-hydroxypentanoic acid is weaker than LA, it is easily replaced by LA before it reacts with the surface-adsorbed H atoms for further dehydration and hydrogenation to produce VA. As 4-hydroxypentanoic acid desorbs from the Pb electrode surface, it subsequently undergoes internal esterification (not an electrochemical reaction) to form the five C-ring compound gVL. With increasing applied

Scheme 1, the ketone radical anion could be stabilized by the neighboring electron-donating CH_3- group, thereby favoring its formation, whereas the lack of CH_3- attached to the aldehyde group of glyoxylic acid makes the intermediate unstable,^[33] leading to the slower reaction rate of glyoxylic acid hydrogenation on Pb. On the other hand, the presence of the two-carbon chain ($-\text{CH}_2-\text{CH}_2-$) allows the dehydration step and subsequent hydrogenation to VA, as demonstrated in Scheme 1a.

The design of the single electrocatalytic (flow) cell reactor and elucidated pathways for ECH of ketone or aldehyde groups reported herein may be extended to remove oxygen contained in the other biomass-related compounds, such as hydroxymethylfurfural (HMF), furfural, and maleic acid, which are abundant from the outlet streams of catalytic conversion of glucose or sorbitols,^[1d,23b,34] allowing their subsequent upgrading processes to fuels or valuable chemicals. Our current research is to rationally design and accurately prepare nanostructured metallic catalysts and fabricate 3D ordered electrodes to further reduce the operation voltage (overpotential) and optimize the reaction pathways, to achieve higher ESE in the single electrocatalytic (flow) cell reactor.

Conclusions

We have reported the ECH of LA to VA or gVL on a non-precious Pb electrode in the single electrocatalytic (flow) cell reactor, with a higher LA conversion, VA yield, Faradaic efficiency, and lower EC than that of a half-cell (batch reactor). This is due to better mass transport resulting from custom-designed and optimized operating conditions in the single electrocatalytic (flow) cell reactor. Meanwhile, renewable electricity can be directly stored in the form of chemical potential energy, as we have demonstrated using the conversion of LA to either VA or gVL. The ESE of 70.8% was achieved by using this new single electrocatalytic (flow) cell electricity storage device. In addition, the applied voltage and electrolyte pH could be used to regulate the product selectivity: lower overpotential or higher electrolyte pH facilitated the formation of gVL, whereas higher overpotential or lower electrolyte pH favored the production of VA. Our pathway investigation on the electrocatalytic reduction of biomass compounds containing ketone or aldehyde groups showed that the molecular structure had a great influence on the reduction rate and final reduction products: VA could be produced through four-electron-transfer electroreduction of LA, whereas the $\text{C}=\text{O}$ group was only reduced to $-\text{OH}$ by a two-electron-transfer process with glyoxylic acid and pyruvic acid as feedstocks. This study may shed light on the rational design of nanostructured catalysts and modification of a single electrocatalytic (flow) cell reactor for the efficient processing of many other renewable, abundant, and cheap oxygen-rich biomass-derived compounds into hydrogen-rich biofuels or biofuel precursors.

Experimental Section

Electrode surface pretreatment: The Pb (Rotometals Inc., United States, 99.9%) and Cu (Small Parts Inc., United States, 99.9%) plates were cut into electrodes with a projected area of 6.5 cm^2 and served as working electrodes in both the half-cell (batch) and single electrolysis (flow) cell reactors. Prior to ECH experiments, the metal electrodes were polished to a mirror finish with sandpaper (320 grits and subsequently 1200 grits) purchased from Leco Corporation. A scanning electron microscope (JEOL JSM-6400) equipped with energy-dispersive X-ray microanalysis (EDS) was used to characterize the surface of the copper and lead electrodes, as shown in Figure S6 in the Supporting Information.

Electrochemical cell configuration: ECH experiments were carried out in both half-cell (batch) and single electrocatalytic (flow) cell reactors at ambient pressure and temperature. The half-cell test was conducted in a conventional three-electrode setup (AFCELL3, Pine Instruments), equipped with an Ag/AgCl (3.5 M KCl, Pine Instrument) reference electrode. The Pt wire counter electrode was placed in a glass tube with glass frits to prevent the diffusion of the products generated on the Pb working electrode. Potential was applied by using a multichannel potentiostat (VersaSTAT MC, Princeton Applied Research). To reduce the solution resistance, the distance between the reference electrode and metal working electrodes was kept small ($<0.5\text{ cm}$).

A custom-made single electrocatalytic (flow) cell reactor was assembled as shown in Figure 5. Pb or Cu electrodes served as the working electrode, which was placed in the cathode chamber, while the Pt foil (thickness 0.5 mm, Aldrich, 99.99% trace metals basis) employed as counter electrode was placed in the anode chamber. Solid-polymer electrolyte membranes, including an anion-exchange membrane (FAA, 110 μm , Fuma-Tech, GmbH) for reduction in a neutral environment and a proton-exchange membrane (Nafion117, Ion Power, Inc.) for reduction in an acid environment, were used to separate the anode and cathode chambers to minimize the cross-over of the products or precursors from the cathode to the anode. The products examined on the anode chamber (OER side) of the cell were of very low concentration: <1 and $<5\%$ after 2 and 20 h of operation, respectively. In addition, the larger electrode area (6.5 cm^2) and small cathode chamber volume (12 mL), along with a fast flow rate of 30 sccm, were optimized to ensure a sufficient LA supply to the Pb electrode surface, while avoiding the mass transport issue resulting from hydrogen gas bubbles striking the Pb electrode.

ECH process: Before the ECH was conducted at constant potentials, cathodic cyclic voltammetry scans were performed for 20 cycles from -0.35 to -1.6 and -0.35 to -1.5 V versus RHE on a Pb electrode in a solution at pH 0 and 7.5, respectively, whereas the scan range was -0.35 to -1.1 V versus RHE on a Cu electrode in a solution of pH 0. The scan rate was 50 mV s^{-1} . The cyclic voltammetry scans were taken to ensure that the surface CuO_x was reduced. The last stabilized CV curve was reported. The upper limits of the cyclic voltammetry scan ranges were selected to be within the potentials at which the dissolution of Pb and Cu metals might occur. Buffer solutions of K_2HPO_4 and KH_2PO_4 with or without the addition of LA were prepared with $18.2\text{ M}\Omega$ deionized water and the pH of this neutral electrolyte was adjusted to 7.5. The acidic electrolyte was prepared by applying the precursors (LA, gVL, pyruvic acid, and glyoxylic acid) in $0.5\text{ M H}_2\text{SO}_4$. The pH of the acidic electrolyte was set to be zero.

As for the ECH conducted in the half-cell (batch) reactor, 55 mL of electrolyte was loaded into three-necked glassware. CA was carried

out to study the potential effect on the product distribution during the ECH process. The ECH was also carried out in a single electrocatalytic (flow) cell reactor. During each run, 55 mL of 0.2 M LA in neutral or acidic electrolyte was introduced into a plastic vessel and pumped into the cathode compartment through a closed loop by a peristaltic pump (Gilson Miniplus 3) at a flow rate of 30 sccm. Meanwhile, H₂SO₄ or K₂HPO₄/KH₂PO₄ buffer solution with the same pH as the cathode reactant solution was cycled through the anode chamber. For both half-cell and single electrocatalytic cell reactors, the applied potential at the cathode was controlled by using a potentiostat (VersaSTAT MC, Princeton Applied Research) and the products at the end of the reaction were collected and analyzed by HPLC. ICP-AES was performed to examine the stability of the Pb electrode after prolonged reaction.

Product analysis: The ECH products were analyzed by HPLC (Agilent 1100) with a refractive index detector (RID; Agilent G1362A) and a variable wavelength detector (VWD; 220 nm, Agilent G1314A). An OA-1000 column (Alltech) was operated at 60 °C and an eluent of 5 mM aqueous sulfuric acid (0.3 mL min⁻¹) was applied to separate the product. A sample volume of 20 µL was injected into the HPLC system. The products were identified by comparison with authentic samples. The Faradaic efficiency was defined by Equation (10):

$$\text{Faradaic efficiency} = \frac{\text{mol}_{\text{specific product}} n F}{I t} \times 100 \% \quad (10)$$

in which n is the number of electrons transferred, F is the Faraday constant, I is the current observed in the experiment, and t is the duration of the experiment. The product selectivity in the liquid phase and carbon (material) balance (CB) were calculated by using Equations (11) and (12):

$$\text{selectivity} = \frac{\text{mol of specific identified product}}{\text{mol of all identified products}} \times 100 \% \quad (11)$$

$$\text{CB} = \frac{\text{mol of carbon in all identified products}}{\text{mol of carbon in initially fed fuels}} \times 100 \% \quad (12)$$

The yield of product was calculated from Equation (13):

$$\text{yield} = \text{selectivity} \times \text{conversion} \quad (13)$$

For the data reported herein, the total and individual carbon balance for each compound was within 5%. A smaller carbon balance means more carbon atoms are accounted for in the product analysis.

Acknowledgements

We acknowledge partial financial support from the US National Science Foundation (CBET-1032547, CBET-1235982) and Michigan Tech Research Excellence Fund (E49290). L.X. acknowledges a Michigan Tech Doctoral Finishing Fellowship and J.Q. is grateful to the Chinese Scholarship Council for support.

Keywords: biofuels • biomass • electrochemistry • energy storage • hydrogenation

- [1] a) S. Chu, A. Majumdar, *Nature* **2012**, 488, 294–303; b) J. Ragauskas, C. K. Williams, B. H. Davison, G. Britovsek, J. Cairney, C. A. Eckert, W. J. Frederick, J. P. Hallett, D. J. Leak, C. L. Liotta, J. R. Mielenz, R. Murphy, R.

- Templer, T. Tschaplinski, *Science* **2006**, 311, 484–489; c) P. V. Kamat, *J. Phys. Chem. C* **2007**, 111, 2834–2860; d) E. L. Kunkes, D. A. Simonetti, R. M. West, J. C. Serrano-Ruiz, C. A. Gartner, J. A. Dumesic, *Science* **2008**, 322, 417–421.
- [2] Challenges of Electricity Storage Technologies, APS Panel on Public Affairs Committee on Energy and Environment **2007**; available from <http://www.aps.org/policy/reports/popa-reports/upload/Energy-2007-Report-ElectricityStorageReport.pdf>.
- [3] a) G. W. Huber, S. Iborra, A. Corma, *Chem. Rev.* **2006**, 106, 4044–4098; b) B. Elvers, *Handbook offuels: Energy Sources for Transportation*, Wiley-VCH, Weinheim, **2008**.
- [4] A. Corma, S. Iborra, A. Vely, *Chem. Rev.* **2007**, 107, 2411–2502.
- [5] a) J. J. Bozell, G. R. Petersen, *Green Chem.* **2010**, 12, 539–554; b) T. Werpy, G. R. Petersen, *Results of Screening for Potential Candidates from Sugar and Synthesis Gas*, **2004**, Vol. 1, US Department of Energy, Washington; c) J. E. Holladay, J. J. Bozell, J. F. White, D. Johnson, *Results of Screening for Potential Candidates from Biorefinery Lignin in Top Value Added Chemicals from Biomass*, **2007**, Vol. 2, US Department of Energy, Washington.
- [6] a) S. W. Fitzpatrick (Biofine Incorporated), World patent 9640609, **1997**; b) P. Gallezot, *Chem. Soc. Rev.* **2012**, 41, 1538–1558.
- [7] D. J. Hayes, S. Fitzpatrick, M. H. B. Hayes, J. R. H. Ross, *Biorefineries—Industrial Processes and Products*, Wiley-VCH, Weinheim, **2008**, pp. 139–164.
- [8] a) L. Deng, Y. Zhao, J. Li, Y. Fu, B. Liao, Q.-X. Guo, *ChemSusChem* **2010**, 3, 1172–1175; b) E. I. Gürbüz, D. M. Alonso, J. Q. Bond, J. A. Dumesic, *ChemSusChem* **2011**, 4, 357–361; c) W. R. H. Wright, R. Palkovits, *ChemSusChem* **2012**, 5, 1657–1667; d) S. G. Wettstein, J. Q. Bond, D. M. Alonso, H. N. Pham, A. K. Datye, J. A. Dumesic, *Appl. Catal. B* **2012**, 117, 321–329.
- [9] a) J. C. Serrano-Ruiz, D. Wang, J. A. Dumesic, *Green Chem.* **2010**, 12, 574; b) J. P. Lange, R. Price, P. M. Ayoub, J. Louis, L. Petrus, L. Clarke, H. Gosse-link, *Angew. Chem.* **2010**, 122, 4581–4585; *Angew. Chem. Int. Ed.* **2010**, 49, 4479–4483.
- [10] J. Q. Bond, D. M. Alonso, D. Wang, R. M. West, J. A. Dumesic, *Science* **2010**, 327, 1110–1114.
- [11] C. H. Zhou, X. Xia, C. X. Lin, D. S. Tong, J. Beltramini, *Chem. Soc. Rev.* **2011**, 40, 5588–5617.
- [12] M. M. Wright, D. E. Dugaard, J. A. Satrio, R. C. Brown, *Fuel* **2010**, 89, S2–S10.
- [13] a) S. H. Langer, H. P. Land, *J. Am. Chem. Soc.* **1964**, 86, 4694–4698; b) S. H. Langer, S. Yurchak, *J. Electrochem. Soc.* **1969**, 116, 1228; c) F. D. Popp, H. P. Shultz, *Chem. Rev.* **1962**, 62, 19–40.
- [14] T. S. Dalavoy, J. E. Jackson, G. M. Swain, D. J. Miller, J. Li, J. Lipkowski, *J. Catal.* **2007**, 246, 15–28.
- [15] P. Nilges, T. R. dos Santos, F. Harnisch, U. Schroeder, *Energy Environ. Sci.* **2012**, 5, 5231–5235.
- [16] E. Troncoso, M. Newborough, *Int. J. Hydrogen Energy* **2011**, 36, 120–134.
- [17] K. W. Harrison, G. D. Martin, T. G. Ramsden, W. E. Kramer, F. G. Novacheck in *The Wind-to-Hydrogen Project: Operational Experience, Performance Testing, and Systems Integration*, **2009**, US Department of Energy-NREL Technical Report, Washington, pp. 1–95.
- [18] Windgas project, Greenpeace Energy, Hamburg, **1986**; available from <http://www.greenpeace-energy.de/service/downloads/windgas.html>.
- [19] M. Gattrell, N. Gupta, A. Co, *J. Electroanal. Chem.* **2006**, 594, 1–19.
- [20] Y. Hori, I. Takahashi, O. Koga, N. Hoshi, *J. Phys. Chem. B* **2002**, 106, 15–17.
- [21] a) A. S. Agarwal, Y. Zhai, D. Hill, N. Sridhar, *ChemSusChem* **2011**, 4, 1301–1310; b) R. Williams, A. Bloom, US Patent 4160816, **1979**; c) Electricity Prices for Industry, US Energy Information Administration, Washington, **2010**; available from <http://205.254.135.24/emeu/international/electricity.html> (accessed August, 2011).
- [22] a) Z. Zhang, L. Xin, J. Qi, Z. Wang, W. Li, *Green Chem.* **2012**, 14, 2150–2152; b) L. Xin, Z. Zhang, Z. Wang, W. Li, *ChemCatChem* **2012**, 4, 1105–1114.
- [23] a) R. Weingarten, J. Cho, R. Xing, W. C. Conner, Jr., G. W. Huber, *ChemSusChem* **2012**, 5, 1280–1290; b) J. Carlos Serrano-Ruiz, R. Luque, A. Sepulveda-Escribano, *Chem. Soc. Rev.* **2011**, 40, 5266–5281.
- [24] D. J. Braden, C. A. Henao, J. Heltzel, C. T. Maravelias, J. A. Dumesic, *Green Chem.* **2011**, 13, 1755–1765.

- [25] S. K. Green, G. A. Tompsett, H. J. Kim, W. B. Kim, G. W. Huber, *ChemSusChem* **2012**, *5*, 2410–2420.
- [26] J. C. Serrano-Ruiz, D. J. Braden, R. M. West, J. A. Dumesic, *Appl. Catal. B* **2010**, *100*, 184–189.
- [27] G. Girishkumar, B. McCloskey, A. C. Luntz, S. Swanson, W. Wilcke, *J. Phys. Chem. Lett.* **2010**, *1*, 2193–2203.
- [28] a) M. S. Dresselhaus, I. L. Thomas, *Nature* **2001**, *414*, 332–337; b) B. C. H. Steele, A. Heinzel, *Nature* **2001**, *414*, 345–352.
- [29] H. A. Gasteiger, N. M. Markovic, *Science* **2009**, *324*, 48–49.
- [30] a) H. A. Gasteiger, S. S. Kocha, B. Sompalli, F. T. Wagner, *Appl. Catal. B* **2005**, *56*, 9–35; b) E. Yeager, *Electrochim. Acta* **1984**, *29*, 1527–1537; c) V. R. Stamenkovic, B. Fowler, B. S. Mun, G. Wang, P. N. Ross, C. A. Lucas, N. M. Markovic, *Science* **2007**, *315*, 493–497; d) L. Carrette, K. A. Friedrich, U. Stimming, *Fuel Cells* **2001**, *1*, 5–39.
- [31] S. W. Lee, C. Carlton, M. Risch, Y. Surendranath, S. Chen, S. Furutsuki, A. Yamada, D. G. Nocera, Y. Shao-Horn, *J. Am. Chem. Soc.* **2012**, *134*, 16959–16962.
- [32] R. Borup, J. Meyers, B. Pivovar, Y. S. Kim, R. Mukundan, N. Garland, D. Myers, M. Wilson, F. Garzon, D. Wood, P. Zelenay, K. More, K. Stroh, T. Zawodzinski, J. Boncella, J. E. McGrath, M. Inaba, K. Miyatake, M. Hori, K. Ota, Z. Ogumi, S. Miyata, A. Nishikata, Z. Siroma, Y. Uchimoto, K. Yasuda, K.-i. Kimijima, N. Iwashita, *Chem. Rev.* **2007**, *107*, 3904–3951.
- [33] T. W. G. Solomons, C. Fryhle, *Organic Chemistry, 10th ed.*, Wiley-VCH, Weinheim, **2009**.
- [34] G. W. Huber, J. N. Chheda, C. J. Barrett, J. A. Dumesic, *Science* **2005**, *308*, 1446–1450.

Received: October 15, 2012

Revised: December 13, 2012

Published online on ■ ■ ■ ■, 0000

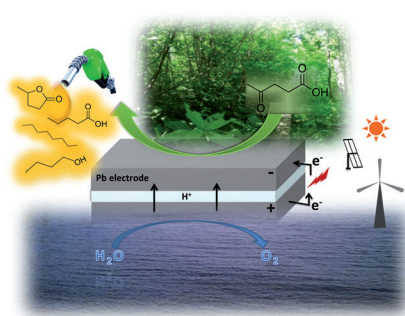
FULL PAPERS

L. Xin, Z. Zhang, J. Qi, D. J. Chadderdon,
Y. Qiu, K. M. Warsko, W. Li*

■■■ – ■■■



Electricity Storage in Biofuels: Selective Electrocatalytic Reduction of Levulinic Acid to Valeric Acid or γ - Valerolactone



Packing a punch! Electricity storage in biofuels by controlled electrocatalytic hydrogenation of levulinic acid to valeric acid or γ -valerolactone on a non-precious Pb electrode in a single electrocatalytic (flow) cell reactor with a high yield, Faradaic efficiency, and electricity storage efficiency, and a low electricity consumption is achieved (see picture). The applied potential and pH value can be used to accurately control the selectivity to valeric acid ($4e^-$ reduction) and γ -valerolactone ($2e^-$ reduction).